Thermodynamic Analyses of a Moderate-Temperature Process of Carbon Dioxide Hydrogenation to Methanol via Reverse Water–Gas Shift with In Situ Water Removal

Cui, Xiaoti; Kær, Søren Knudsen

Published in:
Industrial & Engineering Chemistry Research

DOI (link to publication from Publisher):
10.1021/acs.iecr.9b01312

Publication date:
2019

Document Version
Accepted author manuscript, peer reviewed version

Thermodynamic analyses of a moderate-temperature process of carbon dioxide hydrogenation to methanol via reverse water-gas shift with in situ water removal

Cui Xiaoti, Kær K. Søren*

Department of Energy Technology, Aalborg University, 9220 Aalborg, Denmark

ABSTRACT: CO_2 hydrogenation to methanol via the reverse water gas shift (the CAMERE process) is an alternative way for methanol synthesis. High operating temperatures (600-800°C) are required for the reverse water gas shift (RWGS) process due to the thermodynamic limit. In this study, moderate temperatures (200 – 300°C) were used for the RWGS part in the CAMERE process by the application of in situ water removal (ISWR). Thermodynamic analyses were conducted on this process using the Gibbs free energy minimization method. The analyses show that by using ISWR with high water removal fractions (e.g., 0.80 – 0.99) the CO_2 conversion of the RWGS part can be significantly improved at moderate operating temperatures. The one-step CO_2 hydrogenation to methanol (CTM) with ISWR was also investigated which resulted in similar methanol yields. Both processes showed a high potential and ability to promote CO_2 hydrogenation to methanol through the use of ISWR.

1. Introduction

Carbon capture, utilization, and storage are the major strategies to reduce global CO_2 emissions[1]. The use of carbon dioxide involves the conversion of CO_2 into valuable carbon-based intermediates or end products[2]. In particular, over the last two decades, there has been increasing interest in the direct hydrogenation of CO_2 to oxygenated products, e.g., methanol (MeOH), dimethyl ether (DME), formic acid, and higher alcohols.

Methanol is an important alternative transportation fuel and intermediate for several downstream products, e.g., acetic acid, formaldehyde, DME, olefins, gasoline, and biodiesel[3]. In addition, methanol can be used as a safe and efficient carrier for the storage and transportation of hydrogen[4]. Industrial methanol is mainly derived from syngas (CO is the main source of carbon) at pressures of 50–100 bar and temperatures of 200–300 °C; additionally methanol is derived from the hydrogenation of CO and CO_2 and reverse water–gas shift (RWGS) reactions[5]:

$$CO + 2H_2 \leftrightarrow CH_3OH \qquad \Delta H_{298K} = -91 \text{ kJ/mol} \qquad (1)$$

$$CO_2 + 3H_2 \leftrightarrow CH_3OH + H_2O \qquad \Delta H_{298K} = -49 \text{ kJ/mol} \qquad (2)$$

$$CO_2 + H_2 \leftrightarrow CO + H_2O \qquad \Delta H_{298K} = +41 \text{ kJ/mol} \qquad (3)$$

The one-pass conversion of CO_x (CO and CO_2) to methanol is approximately 5–15% in an industrial process of methanol production (in a fixed bed reactor, e.g., Lurgi type methanol reactor) [6], and the recycling of the unconverted syngas is necessary, and a recycle ratio of 2–5 is typically used for the gas phase process of methanol synthesis.

Compared with the methanol synthesis process from syngas, the hydrogenation of CO_2 or CO_2-rich feed gas (captured from coal-fired power plants, cement plants, and biogas) to methanol generates a larger amount of water byproduct (approximately 30–40% water in crude methanol for the hydrogenation of pure CO_2[7]) which may promotes the deactivation of a conventional copper-

based catalyst via different possible mechanisms[8], e.g., inhibiting effect of water adsorption[9-10], morphology changes and oxidation of the active copper-phase[11]. The water byproduct may also decrease possible coke deposition[12] (on copper-based catalysts) which is not a major deactivation mechanism for a typical gas-phase methanol synthesis process. In addition, with respect to thermodynamics, the less active CO_2 results in a lower conversion of CO_x per pass than that from the hydrogenation of syngas. Therefore, catalysts with higher stabilities and activities are required for the CO_2 hydrogenation. The recent development of new catalysts and industrial demonstrations (e.g., a methanol plant in Iceland) was reviewed in the literature[4,7,13].

One method to improve the one-pass CO_x conversion for the hydrogenation of CO_2 or CO_2-rich feed gas is adding the RWGS process (reaction (3)) before a methanol synthesis reactor to convert part of the CO_2 in the feed gas to CO; then, most of the water generated in the RWGS process can be removed before the methanol synthesis reactor. The additional RWGS process results in less water formation in the downstream methanol synthesis process and consequently decreases the detrimental effect of water on the catalyst for the methanol synthesis. This two-step process of CO_2 hydrogenation to methanol via the reverse water gas shift was presented as the CAMERE process by Joo et al.[14]. The study of the CAMERE process showed an increase of up to 29% in methanol production compared to the process without an RWGS reactor. However, a possible disadvantage of this process is that the endothermic RWGS reaction requires a high operating temperature to achieve a high CO_2 conversion due to the thermodynamic limit, and the high temperature (e.g., 600°C[14]) may increase the complexity of relevant heat integration and affect the total energy efficiency of the process. Anicic et al.[15] compared the CAMERE process with the direct synthesis process of methanol from CO_2 (including two methanol synthesis reactors); the results showed a lower (but not significantly lower) energy efficiency for the CAMERE process

due to the energy needed for the high-temperature RWGS reactor was supplied by natural gas. In addition, the high operating temperatures also raise the requirements for the reactor material.

The application of in situ water removal (ISWR) is a possible way to lower the operating temperature for the RWGS reaction by shifting the thermodynamic equilibrium (according to Le Chatelier's principle), and enable the CAMERE process operated at moderate temperatures. The ISWR process can be achieved by applying membrane reactors and the sorption-enhanced reaction process[16]. The application of membrane reactors (MRs) with ISWR for different processes involving CO_2 hydrogenation has been widely investigated, e.g., methanol synthesis[6, 17–20], DME synthesis[21–24] and methanation process[25], and attractive potentials were shown in the improvement of CO_2 conversion. Less attention has been separately paid to the RWGS process, but it is included as an important side reaction in the aforementioned processes with a system of $CO/CO_2/H_2/H_2O$/fuel and zeolite membranes are suggested[17, 20] for the reactor designs. Recently, Gorbe et al.[20] investigated the permeation of $CO_2/H_2/H_2O$ mixtures using a zeolite A membrane for its application in the CO_2 hydrogenation process to methanol. The experimental results revealed its promising performance in the water-gas separation under the conditions of 100–270 kPa and 160–260 °C, which also indicates the potential of MRs for a moderate-temperature RWGS process.

An alternative method involving ISWR is the sorption-enhanced reaction process (SERP), where H_2O sorbents are added in a reactor to remove the produced water. Similarly, SERP has been investigated in different processes related to CO_2 hydrogenation, e.g., methanol synthesis[16, 26–27], DME synthesis[28], and methanation process[21, 29]. For the RWGS process, Carvill et al.[30] conducted a bench-scale SERP testing at 250°C and 115–480 kPa. The experimental results showed a high CO_2-to-CO conversion (36%) at the low operating temperature, under which the conversion should

be 9.8% for a conventional tube reactor without H_2O sorbents. Jung et al.[31] conducted experimental studies on an adsorptive RWGS reactor at different pressures (5 bar and 10 bar) and temperatures (225℃ and 250℃). The results showed a significantly increase (more than three times higher) of CO_2-to-CO conversion by the application of SERP. Ghodhbene et al. [32] evaluated different zeolites (SOD, LTA-4A, and FAU-13X) for the RWGS process with in situ water removal at 250℃ and 500 kPa. Significant improvement of the CO_2-to-CO conversion was found under the investigated conditions; in particular, the CO production was increased by 60% by using FAU-13X.

It should be noted that the applications of MRs and SERP to the system of $CO/CO_2/H_2/H_2O$/fuel are still at research stage. Regarding the cost issues, there is still lack of cost evaluation for membrane reactor for the RWGS or methanol synthesis process. Comparing with a traditional reactor, the complexity for a membrane reactor may result in a higher cost whereas its smaller size reduce the equipment cost[19]. For the SERP process, it is possible to be realized by a periodic operation. A four-step periodic operation for a sorption-enhanced methanol synthesis process (SE-MeOH) was developed at industrial scale with the considerations of the production cost[27]. The study resulted in an improvement of methanol yield (>7%) and decrease in production capacity (2%) with a competitive methanol production cost. From the viewpoint of energy efficiency, the application of ISWR (MRs and SERP) can provide higher conversions of CO_2, which result in a much lower operating temperature for the RWGS process, or smaller recycling flow rate (i.e., lower energy requirement for recycling compressor) for the methanol synthesis process. For the RWGS process, the lower operating temperature indicate the decrease of energy loss from heat exchange process at high temperatures (e.g., 600℃) and may also decrease the difficulty for the heat integration with other part of the system. Atsonios et al. evaluated the energy requirement for a methanol production system from CO_2 where a membrane reactor was used for the methanol

synthesis process. The results showed a lower power requirement compared with the condition using a traditional methanol reactor.

As mentioned, the applications of in situ water removal via MRs and SERP showed good potential in improving the CO_2 conversion for a moderate-temperature RWGS process. However, to the best of our knowledge, there have been no reports of the application of ISWR to the RWGS reactor in the CAMERE process. In the present study, thermodynamic analyses of the CAMERE process operated at moderate temperatures by the application of ISWR were conducted using the Gibbs free energy minimization method. The effects of the reaction conditions such as the temperature, pressure, feed gas composition (H_2/CO_2 and $CO_2/(CO+ CO_2)$) and H_2O removal fraction (R) were investigated to further understand the applicability and feasibility of this process. Furthermore, the application of ISWR to the process of one-step CO_2 hydrogenation to methanol synthesis (hereinafter referred to as CTM) was also considered to compare with the results of the moderate-temperature CAMERE process.

2. Method

Thermodynamic analysis can provide useful and further insights into the applicability of in situ water removal for the CAMERE process. The method of Gibbs free energy minimization is widely used to predict the thermodynamic equilibrium composition of a reactive system with a given feed composition and reaction conditions[33]. For the gas-phase reaction system in the CAMERE process using the Lagrange multiplier method, the Gibbs free energy minimization for the system can be expressed by the following equations considering each species in the gas phase and the total system[34]:

$$\Delta G_{fi}^{\circ g} + RTln\frac{y_i\hat{\varphi}_i P}{p^{\circ}} + \sum_k a_{ik}\lambda_k = 0 \quad (1)$$

$$\sum_{i=1}^{N} n_i \left(\Delta G_{fi}^{\circ g} + RT ln \frac{y_i \hat{\varphi}_i P}{p^{\circ}} + \sum_{k} a_{ik} \lambda_k \right) = 0 \quad (2)$$

with the following constraint:

$$\sum_{i} n_i a_{ik} = A_k \quad (3)$$

where $\Delta G^{\circ g}_{fi}$ is the standard Gibbs free energy of formation of gaseous species i; y_i is the mole fraction of species i; P and P° are the system pressure and standard state pressure (1 atm), respectively; $\hat{\varphi}_i$ is the fugacity coefficient of species i; n_i is the mole number of species i; λ_k is the Lagrange multiplier; a_{ik} is the number of atoms of the k^{th} element in each molecule of gaseous species i; A_k is the total atomic mass of the k^{th} element in the feed.

Thermodynamic analysis was conducted using the Aspen Plus software. The predictive Soave–Redlich–Kwong (PSRK) model was used as the equation of state. The CAMERE process including two parts (RWGS and methanol synthesis) are shown in Figure 1a. A flow rate of 1 kmol/s was set for CO_x (denote the sum of CO and CO_2) in the feed stream. The conditions for the RWGS part were T = 200 – 1000 °C, P = 1 – 10 bar, H_2/CO_2 = 1 – 8 and $CO/(CO+CO_2)$ = 0 – 0.6 (in the feed gas), whereas typical operating conditions of T = 200 – 300 °C and P = 30 – 70 bar were considered for the methanol synthesis part. The main components in the system were H_2, H_2O, CO, CO_2, and methanol. Methane is only included in section 3.1.1 as a byproduct; other possible byproducts for the methanol synthesis process such as DME, alcohols and paraffins were not considered.

For the two parts in Figure 1a, the Gibbs reactors (RGibbs) were used, and thermodynamic equilibrium states were achieved under the investigated conditions. The ISWR process for each section was modeled by the method reported by Catarina Faria et al.[25], where water in the system and generated in the Gibbs reactors was removed by a sequence of separators (see Figure 1b), and a global value of water removal fraction (R) was given by[25]:

$$R = \frac{\sum_{k=1}^{Z} n_{H_2O,k}}{\sum_{k=1}^{Z} n_{H_2O,k} + n_{H_2O,Z+1}} \quad (4)$$

where $n_{H_2O,k}$ is the mole flow rate of water removed from Separator k, and $n_{H_2O,Z+1}$ is the mole flow rate of water in stream *2* (see Figure 1b). A water removal fraction R can be achieved by adjusting the number of separators Z. For each separator, the split fraction (SF) of water is expressed as follows:

$$SF_i = \frac{n_{H_2O,removal}}{n_{H_2O,removal} + n_{H_2O,out}} \quad (5)$$

where $n_{H_2O,removal}$ is the mole flow rate of H_2O removed from separator i, and $n_{H_2O,out}$ is the mole flow rate of H_2O in the output stream of separator i. In the present study, $SF_1 = SF_2 = \ldots SF_{(Z-1)} = 1$ (i.e., $n_{H_2O,out} = 0$) was established, and only SF_Z was adjusted to achieve a certain R value. The calculated values of Z and SF_Z for all the figures in this study are shown in Table S1–S6, Appendix A. In addition, ISWR was only applied to the RWGS part in the CAMERE process (ISWR was considered for the CTM process in section 3.3).

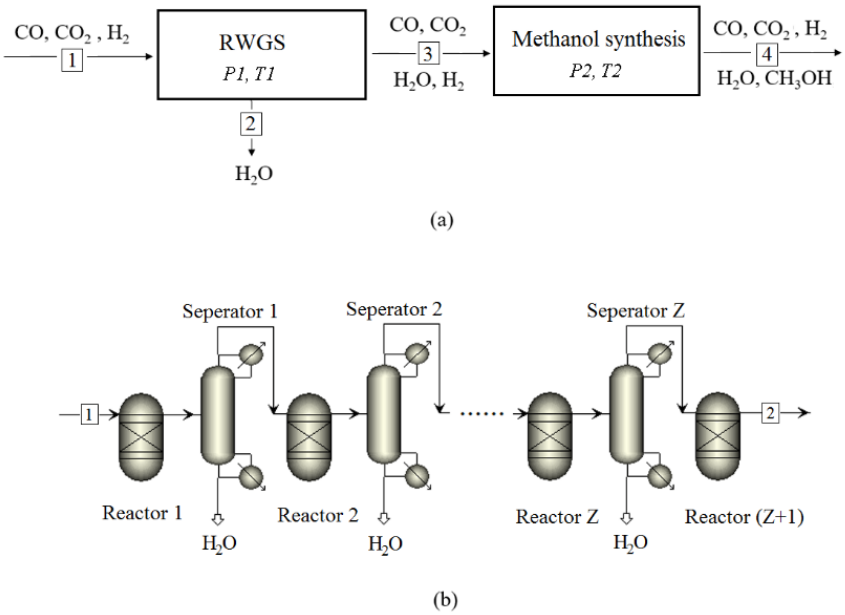

Figure 1. Schemes of (a) the CAMERE process and (b) modular approach for in situ water removal.

As shown in Figure 1a, the conversion of CO_2 for the RWGS (or CAMERE) process can be as follows:

$$C_{CO_2} = \frac{n_{CO_2,1} - n_{CO_2,3(or\ 4)}}{n_{CO_2,1}} \times 100\%, \quad (6)$$

and the methanol yield for the CAMERE (or CTM, Figure 10) process is:

$$Y_{MeOH} = \frac{n_{MeOH,4(or\ 3)}}{n_{CO_2,1} + n_{CO,1}} \times 100\% \quad (7)$$

where the sub index number 1, 3 or 4 represent the stream number in Figure 1a. In addition, only one-pass process was considered for the two parts in Figure 1a; the conditions with a recycle stream for the methanol synthesis process are introduced in section 3.2.3.

3. Results and discussions

3.1 In situ water removal for the RWGS process

3.1.1 Effect of the temperature, pressure and water removal fraction *R*

The thermodynamic analysis for the RWGS process was reported by Kaiser et al.[35], and the equilibrium composition (dry gas) was presented in a large temperature range. Similar trends were obtained in the present study, and the equilibrium composition of water was included as an important component. Figure 2a presents the equilibrium composition for the RWGS reaction at T = 200 – 1000 °C, P = 1.0 bar and H_2/CO_2 = 3 (feed gas), and methane was also considered in the system. The results show that a high operating temperature was required to achieve a high CO_2-to-CO conversion, e.g., when T is 600°C, 700°C and 800 °C, the CO_2-to-CO conversions are 31%, 62% and 73%, respectively. At low temperatures, e.g., T = 200 – 400 °C, little CO is produced, whereas CH_4 and H_2O from the methanation reactions are the main products. However, the application of a copper-based catalyst can improve the CO_2-to-CO conversion at low temperatures because little or no methane is formed in the system via a copper-based catalyst[36]. The equilibrium

composition and CO_2-to-CO conversion without methane in the product are shown in Figure 2b at low temperatures (T = 200 – 300 ℃). The results show higher CO content than those in Figure 2a. However, the CO_2-to-CO conversions remain low in this temperature range, e.g., the CO_2-to-CO conversion is 16% at 250℃.

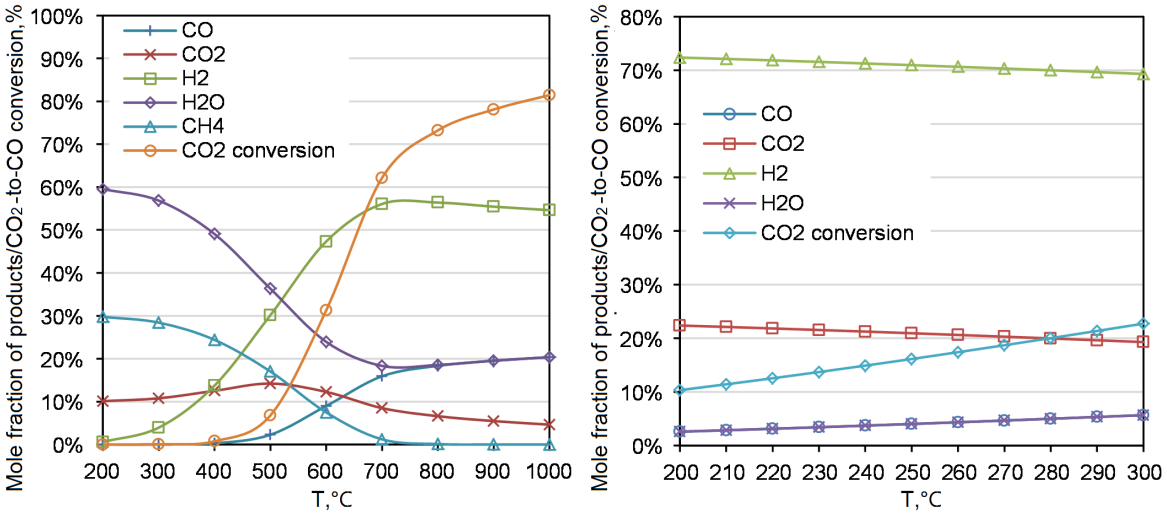

(a) (b)

Figure 2. Equilibrium composition for the RWGS reaction at P = 1.0 bar, H_2/CO_2 = 3 and (a) T = 200 – 1000 ℃ with CH_4 in the product and (b) T = 200 – 300 ℃ without CH_4 in the product.

The operating pressure has no effect on the RWGS reaction because there is no change in volume between the reactants and products[37]. Low operating pressures were selected for the RWGS process in the present study because the methanol synthesis reactions (reaction (1) and (2)) are promoted at high pressures (e.g., P = 50 – 70 bar for a conventional methanol synthesis process). The effect of the methanol synthesis reactions at low pressures was calculated at T = 250℃ and P = 1 – 10 bar (similar to the pressure in the literature[10, 31]) and H_2/CO_2 = 3 (feed gas). The results (data not shown) of the equilibrium composition show little change with the increasing pressure, and a small amount of methanol was formed, e.g., MeOH% = 0.41 mol% with P = 10 bar and MeOH% = 0.11 mol% with P = 5 bar. In the following sections, P or $P1$ = 5 bar was selected for the RWGS process or the RWGS part for the CAMERE process in Figure 1a. It should be noted

that higher operating pressures may be used in industry with different considerations, e.g., for a smaller reactor size.

With the in situ water removal by MRs or SERP, the CO_2-to-CO conversions in Figure 2b can be further enhanced. The water removal fraction R was used to evaluate the extent of water removed from the system; In the work by Catarina Faria et al.[25], the ranges of $0 < R < 0.99$ and $R \geq 0.99$ were assumed for MRs and SERP, respectively. In the present study, the range of $R = 0 – 0.99$ was investigated for the RWGS process. Figure 3a illustrates the equilibrium CO_2-to-CO conversion at different temperatures and R values. The conversion increased with an increase in R, and similar trends were found at different operating temperatures. The promotions are more obvious in high-R zones; for example, C_{CO_2} = 77% was achieved with R = 0.99 and T = 250℃, and the operating temperature without ISWR ($T0$) must be more than 800℃ (dash line in Figure 3) to achieve this conversion. This trend indicates that it is possible to operate the RWGS reactor at moderate temperatures by the application of ISWR, but a high R value is required, e.g., to achieve similar CO_2 conversions from a conventional RWGS reactor in the CAMERE process, $R > 0.80$ (T = 250℃) is required for $T0$ = 600 ℃ values and $R > 0.97$ for $T0$ = 700 ℃.

The high requirement of the R value can be fulfilled by SERP according to the experimental studies in the literature[30–32], for the application of MRs experimental investigations are still required. In the following sections only the high values of $R = 0.80 – 0.99$ were considered. In addition, the equilibrium composition for the RWGS process at 250℃ and different R values is shown in Figure 3b. A significant change of the equilibrium composition was also found for the high-R zone, e.g., CO% increased from 8% to 24% and CO_2% decreased from 18% to 7% when R increased from 0.80 to 0.99. It should be noted that a lower CO_2 content (CO_2% < 7%) can be achieved when R is higher than 0.99, and attention should be paid to the influence of the low CO_2

concentration on the subsequent methanol synthesis process. The promoting effect of a low CO_2 concentration (e.g., 2–5 Vol%[38]) on the rate of methanol synthesis was reported in literatures[39–40], and the reaction rate was obviously reduced when CO_2 was removed from the feed gas[40].

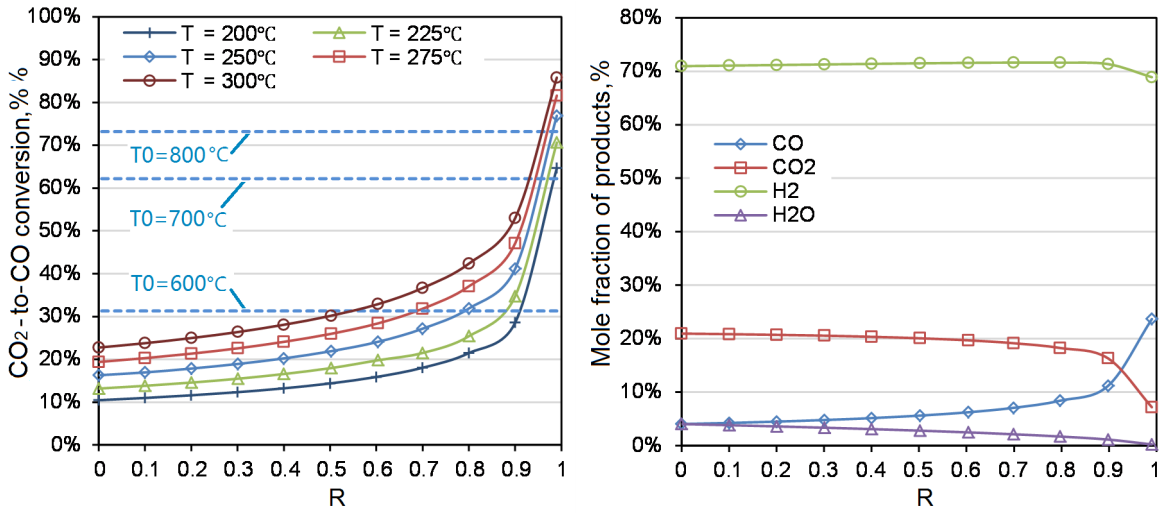

(a) (b)

Figure 3. (a) Equilibrium CO_2-to-CO conversion at different temperatures and *R* values. (b). The equilibrium composition for the RWGS process at 250℃ and different *R* values.

3.1.2 Effect of the feed gas composition

The design feed composition for the CAMERE process is at the stoichiometric molar ratio (H_2/CO_2 = 3); this ratio can vary in different conditions (e.g., feed gas from different sources and mixing with a possible gas recycle from downstream[10]). Figure 4a presents the equilibrium CO_2-to-CO conversion at 250 ℃, different *R* values and H_2/CO_2 ratios (in the feed gas). The condition without in situ water removal (*R* = 0) was included for comparison. The conversion values increased with an increase in H_2/CO_2 ratio, and these promotions were slightly lower for the conditions with high *R* values. For example, when the H_2/CO_2 ratio increased from 1 to 3, the conversion values increased by 70% (*R* = 0), 65% (*R* = 0.90) and 51% (*R* = 0.99). Also, a CO_2-to-CO conversion of 36% was reported under the condition of 250℃, 480 kPa and feed gas of CO_2/H_2=1[30], the corresponding *R* value can be evaluated as 0.9 – 0.99 in Figure 4a. In addition,

the effect of CO in the feed gas was investigated. Figure 4b shows the CO_2 conversion with different *R* values and $CO/(CO+CO_2)$ feed gas compositions. The stoichiometric ratio of $(H_2-CO_2)/(CO+CO_2) = 2$ was set for H_2 in the feed gas. As a product, an increase in CO fraction in the feed gas shifted the equilibrium of the RWGS reaction to the reactant side. Therefore, an obvious decrease of the CO_2-to-CO conversion was found with an increasing $CO/(CO+CO_2)$ ratio. This decrease trend is more obvious at low *R* values; however, for the condition of $R = 0.99$, the decrease trend of the conversion value is not significant due to the strong promotion by the in situ water removal.

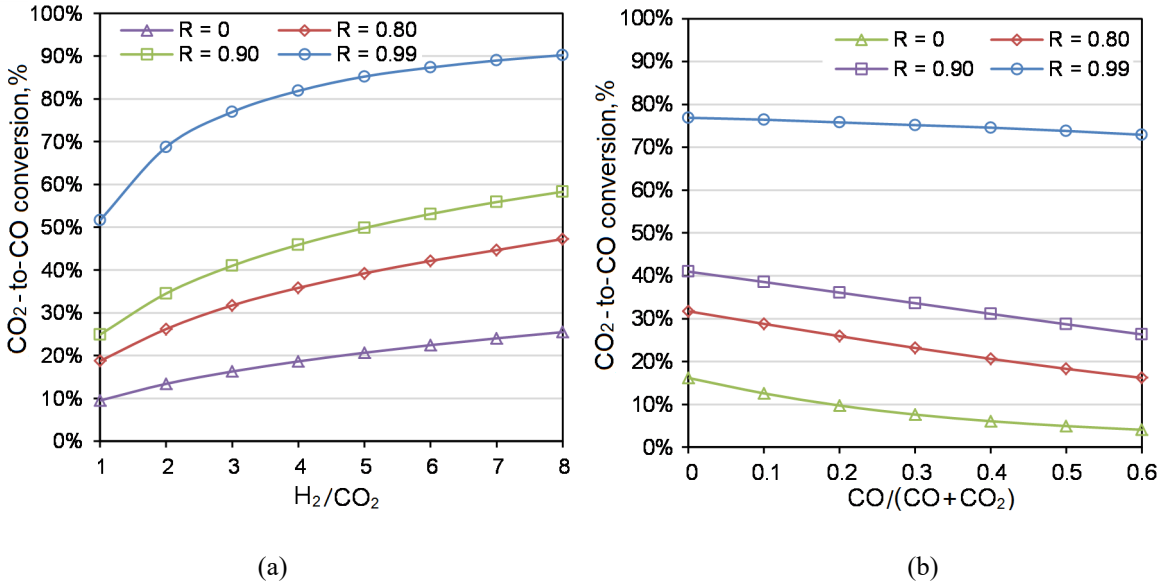

(a) (b)

Figure 4. Equilibrium CO_2-to-CO conversion at 250 °C and different *R* values, (a) H_2/CO_2 ratios and (b) ratios in the feed gas.

3.2 In situ water removal for the CAMERE process

3.2.1 Effect of the temperature, pressure and water removal fraction *R*

As mentioned in section 3.1.1, the in situ water removal for the RWGS process significantly improved the CO_2-to-CO conversion (at low operating temperatures). Then, the ISWR application was investigated for the CAMERE process where the MeOH synthesis part was added with typical operating conditions of *T2* = 250 °C and *P2* = 30 – 70 bar. The effect of *T1* for the RWGS process

was also considered with a range of *T1* = 200 – 300 °C. The stoichiometric molar ratio of H_2/CO_2 = 3 was set for the feed gas (stream 1 in Figure 1a). In addition, the product (stream 3 in Figure 1a) after the RWGS process was cooled to 40 °C and passed through an ideal gas/liquid separator (not shown in Figure 1), and only the gas phase flowed into the methanol synthesis part.

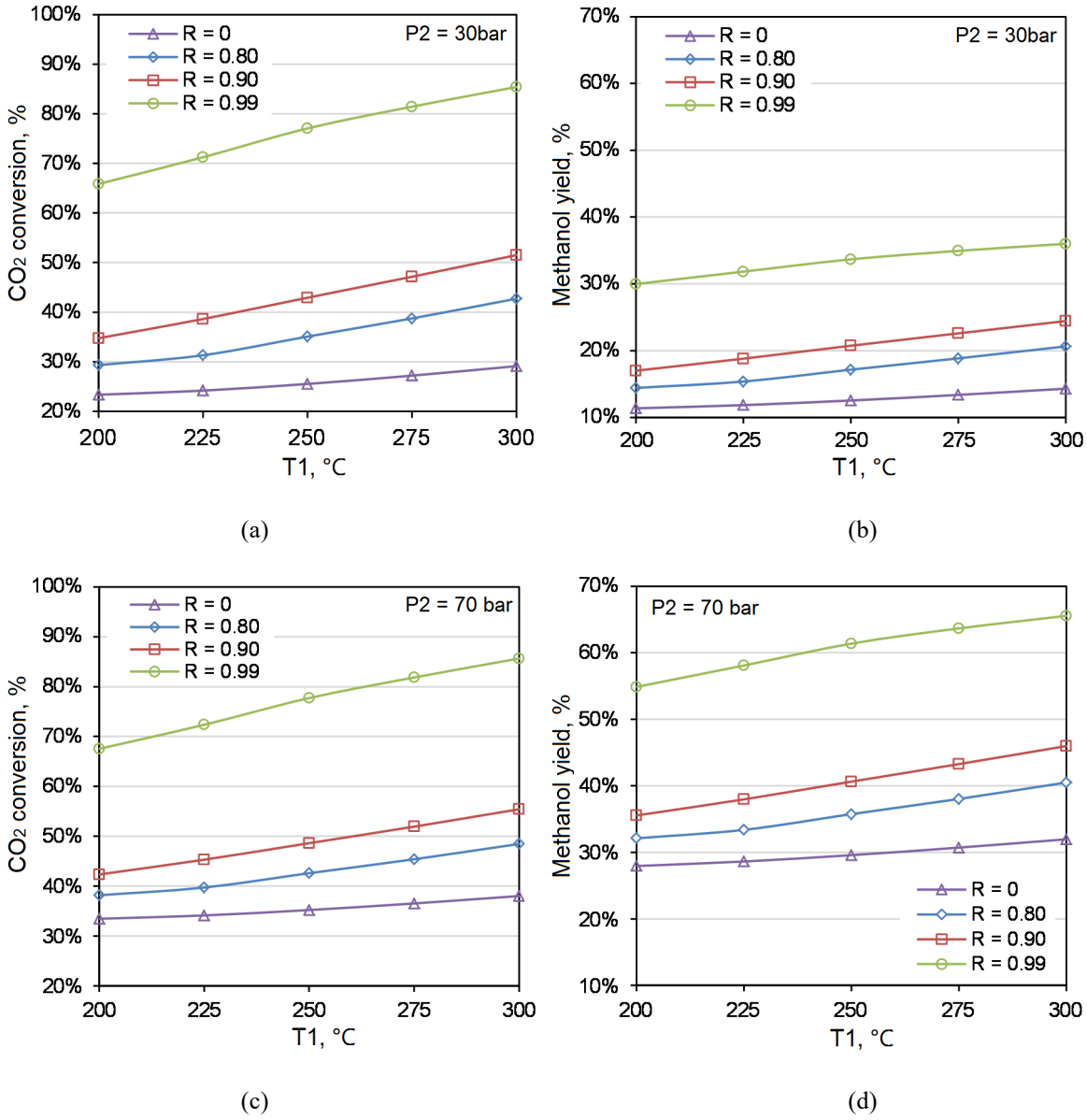

Figure 5. Equilibrium CO_2 conversion (left column) and methanol yield (right column) for the CAMERE process at different *T1* and *R* values (for the RWGS part) and *P2* for the MeOH synthesis part.

Figure 5 illustrates the equilibrium CO_2 conversion and methanol yield for the CAMERE process at different *T1* and *R* values (for the RWGS part) and *P2* (for the MeOH synthesis part) due to their significant effect on the MeOH synthesis reactions[41]. The results show that the CO_2 conversion of the CAMERE process increases with increasing temperature *T1*, which is similar to the trend in Figure 3a for the RWGS process because the RWGS reaction favors high operating temperatures, and more CO generated from the RWGS reaction results in higher methanol yields as shown in Figures. 5b and 5d.

Compared with the condition of $R = 0$, both CO_2 conversion and methanol yield for the CAMERE process were obviously promoted by ISWR. For example, at *T1* = 250℃ and *P2* = 30 bar, when *R* increased from 0 to 0.90, C_{CO_2} increased from 26% to 43%, and Y_{MeOH} increased from 13% to 21%. In particular, the condition with $R = 0.99$ resulted in significant promotions, with C_{CO_2} = 77% and Y_{MeOH} = 34%. The increase in *P2* promoted the CO_2 conversion, and this trend is more obvious for the conditions with lower *R* values. At $R = 0.99$, the product gas from the RWGS part already contained a high level of CO (e.g., CO% is 75% at *T1* = 250℃), and the CO_2 conversion very slightly changed with *P2*. For example, at *T1* = 250℃, the C_{CO_2} values are 77% and 78% at *P2* = 30 bar and 70 bar, respectively, which indicates that there is little promotion of the CO_2 conversion by *P2* when the CO content before the methanol synthesis part is high. In addition, the methanol yield was enhanced by higher *P2* values under the investigated conditions due to the methanol synthesis reactions favors high pressures. Consequently, by using ISWR with high *R* value, a high methanol yield can be achieved at the moderate *T1* values, e.g., Y_{MeOH} = 61% with *T1* = 250℃, *P2* = 70 bar and $R = 0.99$, which is much higher than those for the CTM process (e.g., Y_{MeOH} = 26% with *T1* = 250℃ and *P2* = 70 bar). The conditions with *P2* = 50 bar were also calculated and shown in Figure S1, Appendix A.

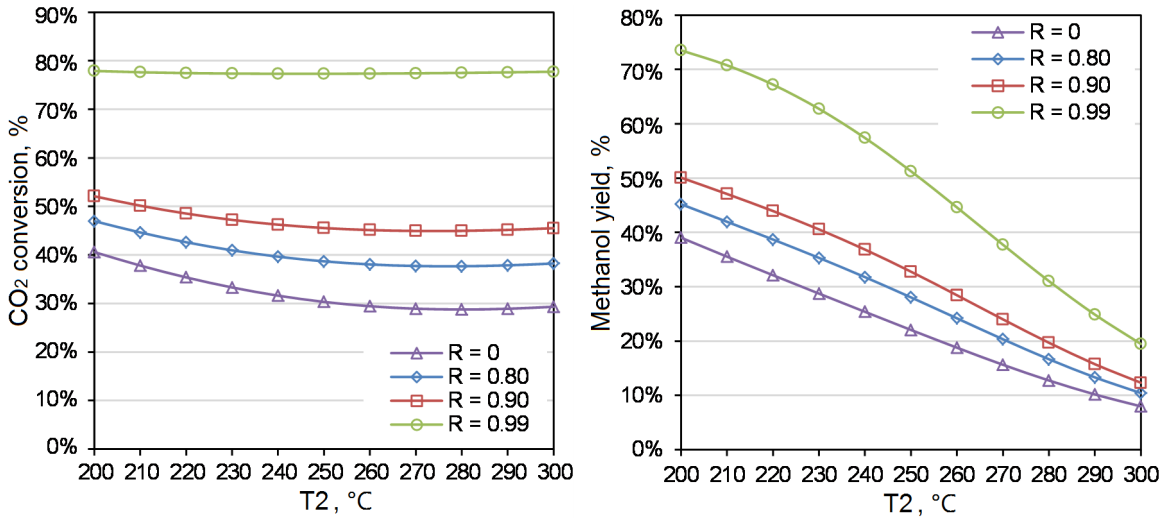

(a) (b)

Figure 6. Equilibrium (a) CO_2 conversion and (b) methanol yield at *T1* = 250°C, *P2* = 50 bar and different *T2* and *R* values.

Besides the temperature for the RWGS part, the temperature for the MeOH synthesis part was also considered. Figure 6a presents the equilibrium CO_2 conversions at different *T2* and *R* values. With $R = 0 - 0.90$, higher CO_2 conversions were found at low temperatures because low temperature is favorable for the exothermic methanol synthesis reactions (reactions (1) and (2)). At high temperatures, the CO_2 conversions were slightly enhanced by the RWGS reaction (reaction (3) occurred in the methanol synthesis reactor), which is consistent with the trends in the work by Stangeland et al. [41]. The trend varies for $R = 0.99$, where the effect of *T2* on the CO_2 conversion is not obvious. This difference could be attributed to the high CO_2 conversion and CO content (also mentioned in Figure 5) after the RWGS part (stream 3 in Figure 1a), and the more active CO component is the main reactant consumed in the MeOH synthesis part. In addition, the equilibrium methanol yield at different *T2* and *R* values is shown in Figure 6b. The decrease in methanol yield with increasing *T2* was found under all conditions due to the negative effect of high temperatures on the methanol reactions, which indicates that although the methanol yield can be promoted by high *R* values, the operating temperature for the MeOH synthesis significantly affects the methanol

yield, e.g., with R = 0.99, Y_{MeOH} decreased from 57% to 38% when *T2* increased from 240℃ to 270℃, which also indicates the importance of the *T2* for the methanol synthesis process and the CAMERE process.

3.2.2 Effect of the feed gas composition

The effect of the H_2/CO_2 ratio in the feed gas (stream 1 in Figure 1a) was also investigated for the CAMERE process. The equilibrium CO_2 conversion (data not shown) increased with the H_2/CO_2 ratio, which is very similar to that for the RWGS process in section 3.1.2. In addition, a higher H_2/CO_2 ratio can shift the equilibrium of the methanol synthesis reactions to the product side. Figure 7a presents the equilibrium methanol yield with different R values and H_2/CO_2 ratios in the feed gas. The methanol yield significantly increased with the increase in H_2/CO_2 ratio under the investigated conditions, and a high methanol yield was achieved with high R and H_2/CO_2 values, e.g., Y_{MeOH} is 67% when R = 0.99 and H_2/CO_2 = 5. The effect of CO in the feed gas was also considered. Figure 7b shows the equilibrium methanol yield with different R values and $CO/(CO+CO_2)$ feed gas compositions for the CAMERE process. The stoichiometric ratio of $(H_2-CO_2)/(CO+CO_2) = 2$ was set for H_2 in the feed gas. The higher CO content in the feed gas promoted the methanol synthesis process and consequently the methanol yield for the CAMERE process. The trend is more obvious at lower R values, e.g., with R = 0.80, Y_{MeOH} is 28% and 46% when $CO/(CO+CO_2)$ is 0 and 0.6, respectively. At high R values, the CO content after the RWGS part (section 3.1.2) was not significantly affected by the CO content in the feed gas, so there was less effect of the $CO/(CO+CO_2)$ ratio on the methanol yields.

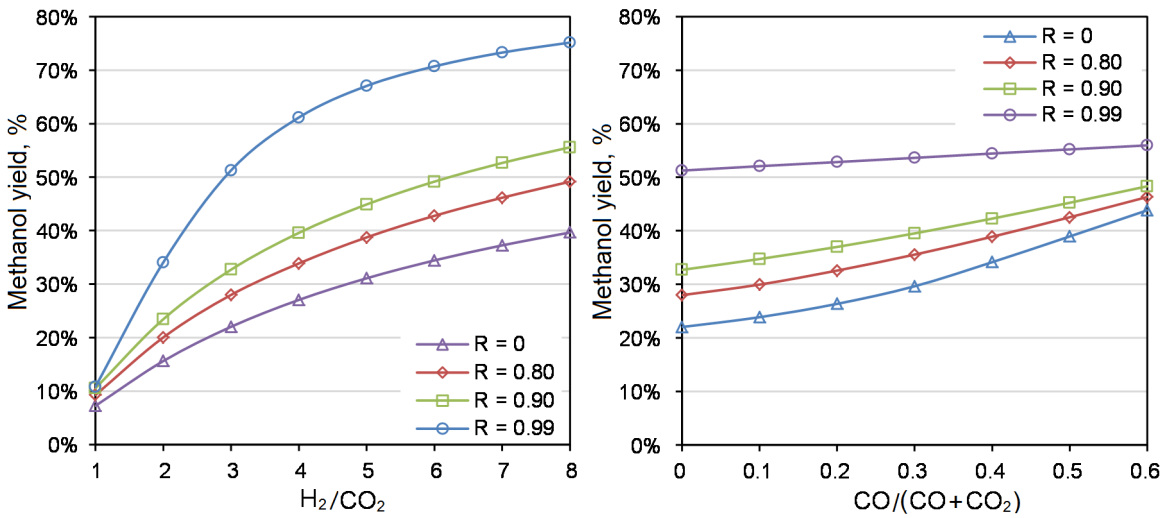

(a) (b)

Figure 7. Equilibrium methanol yield at *T1* = *T2* = 250°C, *P2* = 50 bar and different *R* values, (a) H_2/CO_2 ratios and (b) $CO/(CO+CO_2)$ ratios in the feed gas.

3.2.3 Recycle ratio for the MeOH synthesis process

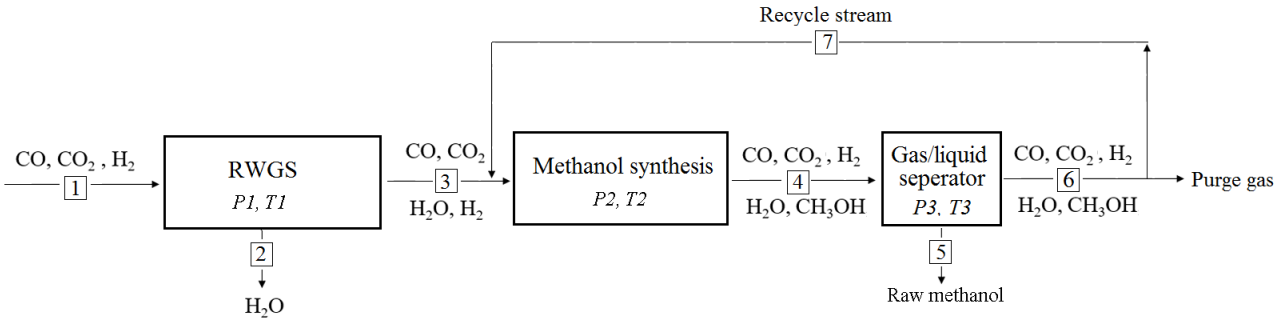

Figure 8. Block scheme of the CAMERE process with ISWR and the recycle stream.

A typical process of CO_2 hydrogenation to methanol requires the recycling of the unconverted feed gas with certain recycle ratios (*N*, mole ratio of recycled stream/feed gas) due to the low one-pass conversion of this process. A lower recycle ratio indicates a lower system load, e.g., a decrease in size of the reactor and recycle gas compressor results in a decrease in investment and energy consumption of the system. As shown in Figure 8, the components of methanol and water in stream 4 were further condensed and separated through an ideal gas/liquid separator at *T3* = 40 °C and *P3*

= 50 bar. A portion of the gas from the separator was purged, and the remainder returned to MeOH synthesis process as the recycle stream (stream 6). The amount of the purged gas was adjusted to achieve different *N* values. Figure 9 presents the equilibrium recycle ratios with different *T2*, *P2* and *R* values for the methanol synthesis in the CAMERE process. The recycle ratio *N* decreased with the decrease in *T2* and increase in *P2* under the investigated conditions. *N* decreased with increasing *R*, and this trend is more obvious at *R* = 0.99, e.g., at *T2* = 250°C and *P2* = 50 bar, *N* is 6.0 and 3.9 when *R* is 0 and 0.99, respectively. In addition, these results indicate that lower recycle ratios can be achieved in the CAMERE process than in a conventional CTM process (the *N* value is close to that with *R* = 0), and the recycle ratio can be further decreased by using ISWR with high *R* values.

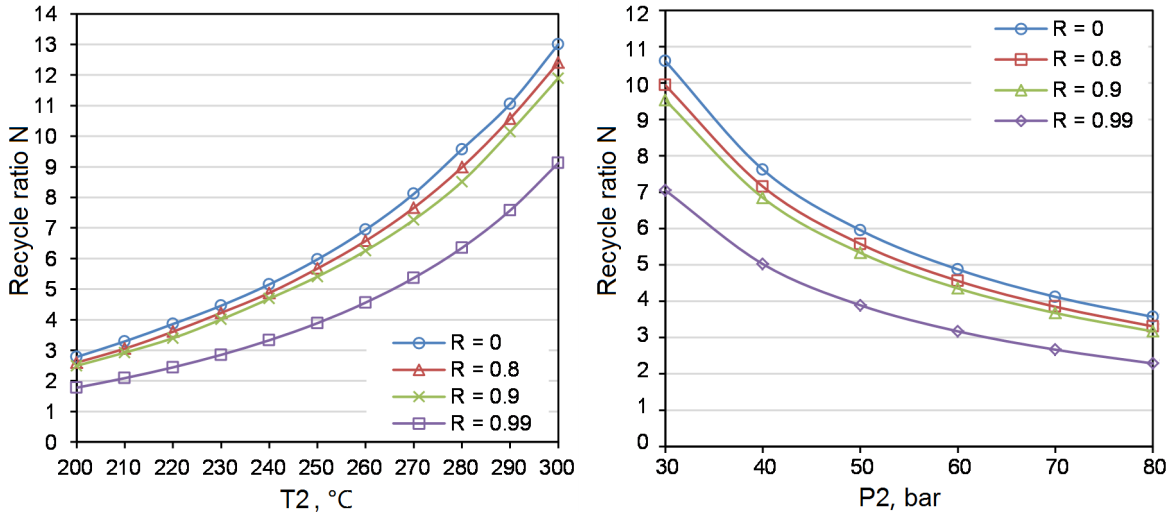

(a) (b)

Figure 9. Equilibrium recycle ratios at *T1* = 250°C and different *R* values, (a) *T2* and (b) *P2* for the MeOH synthesis part in the CAMERE process.

3.3 In situ water removal for the CTM process

In addition to the CAMERE process with ISWR in the above investigations, the application of ISWR to the MeOH synthesis process is also a potential method to improve the CO_2 conversion for the CAMERE process[42] or CTM process[6], because water is one of the main products of reaction

(2). Although the thermodynamic analyses for the CTM process with ISWR have been reported in the literature[6, 18], the effects of ISWR by using the water removal fraction (R) for the CTM process are presented in this study to further compare with the above results for the CAMERE process. The RWGS part was removed from the CAMERE process as shown in Figure 10, for the CTM process, and the method in Figure 1b was used to calculate the ISWR process.

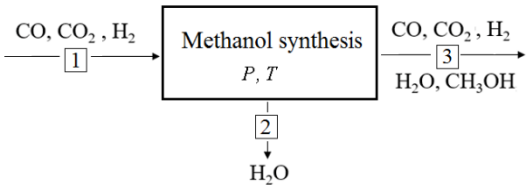

Figure 10. Scheme of the CTM process with ISWR.

Figure 11 presents the equilibrium CO_2 conversion and methanol yield for the CTM process at different temperatures (200 – 300℃), pressures (30 – 70 bar) and R values (0.80 – 0.99). The effects of the operating temperature for the CTM process are similar to the trends for the CAMERE process in Figure 6. For the operating pressure, both CO_2 conversion and methanol yield were promoted by high pressures. These trends are more obvious for the conditions with lower R values, e.g., when the pressure increased from 30 bar to 70 bar (at 250℃), the CO_2 conversion increased by 51%, 26% and 7% for R of 0, 0.90 and 0.99, respectively. Similar to the trends for the CAMERE process, significant improvements of CO_2 conversion and methanol yield by high R values were found under the investigated conditions, which indicates that a lower operating pressure can be used for the CTM process by applying the in situ water removal. For example, at T = 250℃, a higher Y_{MeOH} (34%) was achieved at a lower P (30 bar) and R = 0.99, whereas Y_{MeOH} is 26% at P =70 bar and R = 0 (without ISWR). The conditions with $P2$ = 50 bar were also calculated and shown in Figure S2, Appendix A.

The effect of the H_2/CO_2 and $CO/(CO+CO_2)$ ratio in the feed gas were also investigated for the CTM process (shown in Figure 12). The trends of the equilibrium methanol yield are similar to those for the CAMERE process in Figure 7, and the methanol yield increased with the increases in both H_2/CO_2 and $CO/(CO+CO_2)$ ratios. Compared with the results of the CAMERE process, the methanol yields of the CTM process were slightly higher under the investigated conditions (except the conditions where R = 0). The promotions by ISWR remained obvious for different H_2/CO_2 ratios and low $CO/(CO+CO_2)$ ratios, and high Y_{MeOH} can be achieved (e.g., Y_{MeOH} is 72% when H_2/CO_2 is 5).

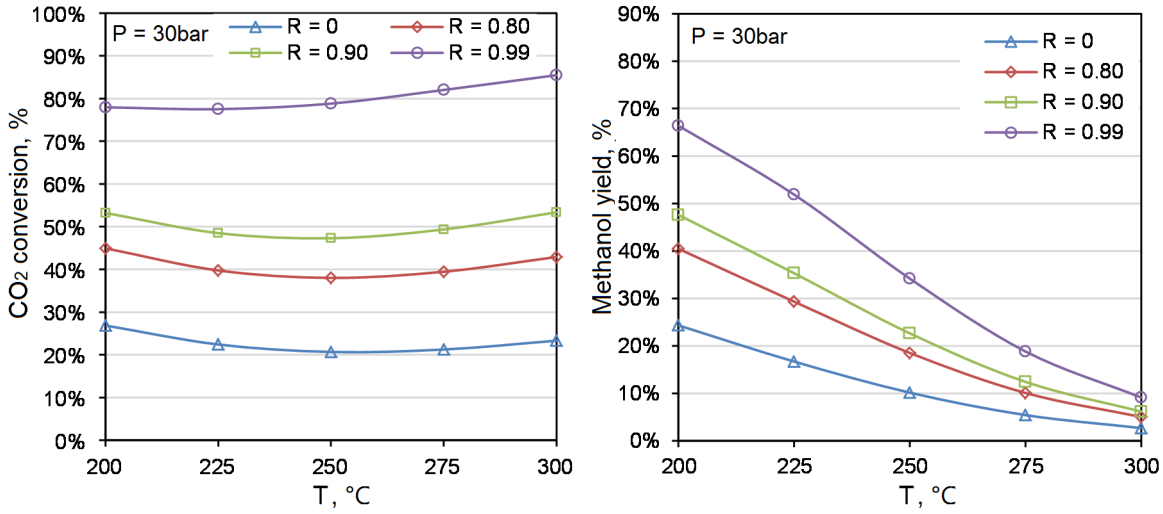

(a) (b)

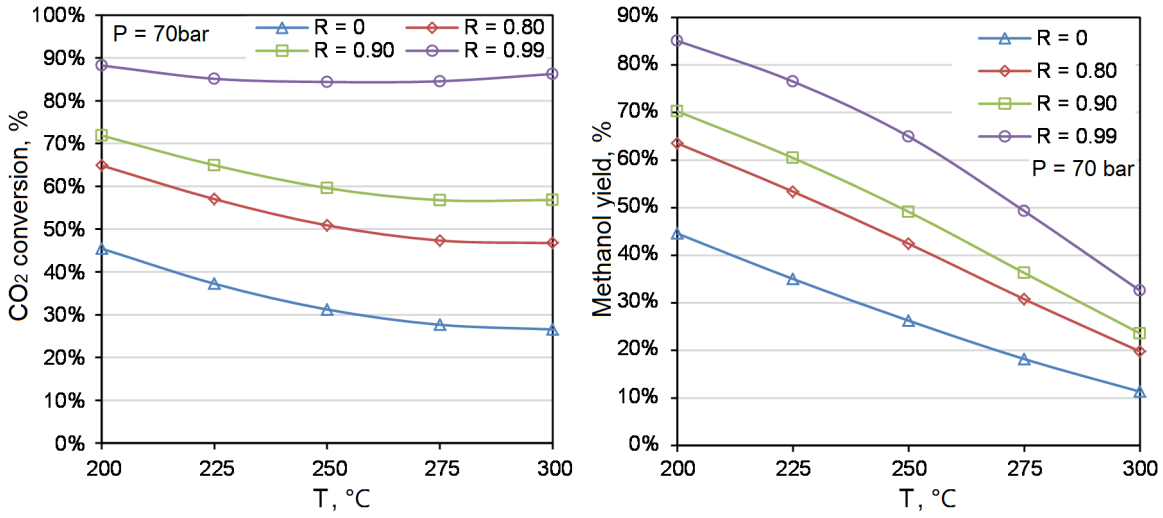

(c) (d)

Figure 11. Equilibrium CO_2 conversion (left column) and methanol yield (right column) for the CTM process under the conditions with H_2/CO_2 = 3(feed gas), T = 200 – 300 ℃, P = 30 – 70 bar and R = 0 – 0.99.

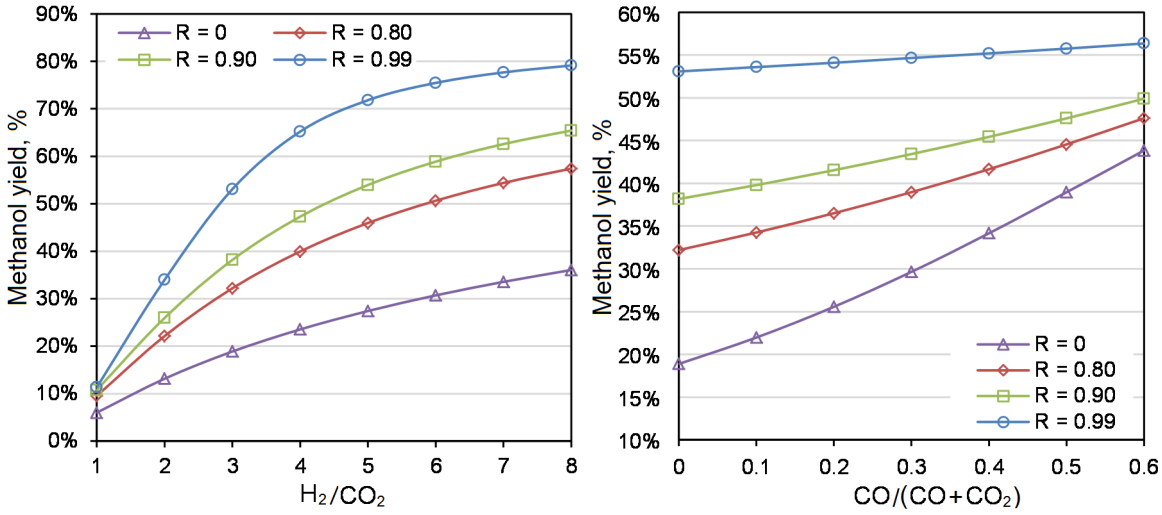

(a) (b)

Figure 12. Equilibrium methanol yield at T = 250℃, P = 50 bar and different R values, (a) H_2/CO_2 ratios and (b) $CO/(CO+CO_2)$ ratios in the feed gas for the CTM process.

3.4 Comparison of the CAMERE and CTM processes with ISWR

Compared with a conventional CTM process, the CAMERE process including a high-temperature RWGS reactor can achieve higher CO_2 conversion and methanol yield (see Figure S3, Appendix A). In the present study, the application of ISWR can promote both processes as

mentioned above, which results in a moderate-temperature CAMERE process and a CTM process with high methanol yields. Figure 13 shows the ratio of the methanol yields between the two processes under identical conditions (P = $P2$ = 50 bar and T = $T2$ = 250℃) for the methanol synthesis process (for both processes) and different $T1$ and R. The $Y_{MeOH,\ CAMERE}$ / $Y_{MeOH,\ CTM}$ ratio increased with $T1$ due to the RWGS reaction favors high temperature, and higher methanol yield can be achieved by a higher $T1$. The CAMERE process showed 9% – 29% higher methanol yield without the application of ISWR (R = 0), whereas the CTM process showed better (not significant) methanol yields for most of the conditions with ISWR (R = 0 – 0.99). Similar trends (data not shown) were also found for the CO_2 conversions and the methanol yields under other pressure conditions (i.e., P = $P2$ = 30 bar and 70 bar).

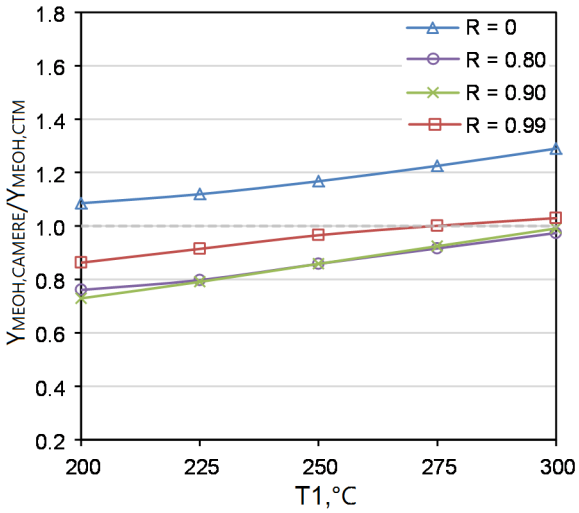

Figure 13. The ratio of the equilibrium methanol yields for the CAMERE and CTM processes under the conditions with H_2/CO_2 = 3(feed gas), R = 0 – 0.99, $T1$ = 200 – 300 ℃, T = $T2$ = 250 ℃ and P = $P2$ = 50 bar.

The pros and cons of the two processes are as follows: (1) For the CAMERE process with ISWR, the water removal only occurred in the RWGS part (in the present study), and there is less detrimental effect of water on the catalyst for the methanol synthesis part. In addition, the RWGS operate at low pressures (e.g., 5 bar), which indicates lower requirements of reactor materials (e.g.,

membranes for water removal) for the water removal process. Furthermore, only a small (or negligible) amount of methanol was generated in the RWGS process, which resulted in a simpler water removal process mainly with the $CO/CO_2/H_2/H_2O$ system. The disadvantage of the CAMERE process is that the RWGS part increases the system complexity and cost with additional RWGS reactors. (2) For the CTM process with ISWR, a simpler system with only the methanol synthesis part is included. The disadvantage of this process can be the higher operating pressure (e.g., 50 bar), which results in higher requirements of reactor materials. In addition, the produced water may still affect part of the catalyst in the methanol synthesis reactor.

4. Conclusions

Thermodynamic analyses were conducted on a moderate-temperature CAMERE process and CTM process by the application of ISWR using the Gibbs free energy minimization method. The operating conditions of T = 200 – 1000 °C, P = 1 – 10 bar, feed gases of H_2/CO_2 = 1 – 8 and $CO/(CO+CO_2)$ = 0 – 0.6 and R = 0 – 0.99 were considered for the RWGS part, whereas the operating conditions of T = 200 – 300 °C and P = 30 – 70 bar were included for the MeOH synthesis in both processes.

For the moderate-temperature CAMERE process, in the investigated temperature and pressure ranges, the application of ISWR can significantly improve the CO_2 conversion of the RWGS part at moderate operating temperatures, which may further decrease the difficulty in relevant heat integration and increase the energy efficiency for this process (compared with the condition without ISWR). High R values (e.g., $R \geqslant 0.80$) are required for the ISWR process to achieve similar CO_2 conversions (31% – 73%) from the conventional CAMERE process with a high-temperature RWGS reactor. The conditions with R = 0.99 showed high CO_2 conversions (e.g.,

77%) and high methanol yields (e.g., 51%). The CTM process showed better (not significant) methanol yields for most of the conditions with ISWR ($R = 0 – 0.99$) under identical conditions ($P = P2 = 50$ bar and $T = T2 = 250$℃) for the methanol synthesis process. From a thermodynamic viewpoint, both processes show a high potential and ability to promote CO_2 hydrogenation to methanol by the application of ISWR.

ASSOCIATED CONTENT

Supporting Information. Equilibrium CO_2 conversion and methanol yield for the CAMERE process at different *T1*, *R* values and $P2 = 50$ bar. Equilibrium CO_2 conversion and methanol yield for the CTM process at different *T*, *R* values and $P2 = 50$ bar. Equilibrium methanol yield for the high-temperature CAMERE process and the CTM process. Calculated values of *Z* and SF_Z for the figures in this study.

AUTHOR INFORMATION

Corresponding Author

*Tel.: +45-2667-8192. E-mail: xcu@et.aau.dk

ORCID

Xiaoti Cui: 0000-0001-6514-0280

Notes

The authors declare no competing financial interest.

Acknowledgment

The authors would like to acknowledge the support of this work from the Danish Energy Agency (EUDP, 64017-0026) funded project Cryogenic Carbon Capture and Use ― C3U.

References

(1) Carbon capture, utlization, and storage: Climate change, economic competitiveness, and energy security. US Department of Energy; 2016.

(2) Styring P, Quadrelli EA, Armstrong K. Carbon dioxide utilization: Closing the Carbon Cycle. Amsterdam: Elsevier; 2014.

(3) Rostrup-Nielsen JR, Christiansen LJ. Concepts in syngas manufacture. London: Imperial College Press; 2011, p. 117.

(4) Gallucci F. Inorganic Membrane reactors for methanol synthesis. In: Methanol: science and engineering. Amsterdam: Elsevier; 2017, p. 493–518.

(5) Bozzano G., Manenti F. Efficient methanol synthesis: Perspectives, technologies and optimization strategies. Progress in energy and combustion science. 2016; 56: 71–105.

(6) Barbieri G, Marigliano G, Golemme G, Drioli E. Simulation of CO_2 hydrogenation with CH_3OH removal in a zeolite membrane reactor. Chem Eng J 2002; 85: 53–59.

(7) Bertau M., Offermanns H., Plass L., Schmidt F., Wernicke HJ. Methanol: The Basic Chemical and Energy Feedstock of the Future. Heidelberg: Springer, 2014.

(8) Bukhtiyarova M, Lunkenbein T, Kähler K. Robert Schlög. Methanol synthesis from industrial CO_2 sources: A contribution to chemical energy conversion. Catal lett 2017; 147: 416–427.

(9) Sahibzada M, Metcalfe IS, Chadwick D. Methanol synthesis from $CO/CO_2/H_2$ over $Cu/ZnO/Al_2O_3$ at differential and finite conversions. J Catal 1998; 174: 111–118.

(10) Arena F, Barbera K, Italiano G, Bonura G, Spadaro L, Frusteri F. Synthesis, characterization and activity pattern of Cu–ZnO/ZrO2 catalysts in the hydrogenation of carbon dioxide to methanol. J Catal 2007; 249: 185-194.

(11) Omata K, Hashimoto M, Watanabe Y, Umegaki T, Wagatsuma S, Ishiguro G, Yamada M. Optimization of Cu oxide catalyst for methanol synthesis under high CO_2 partial pressure using combinatorial tools. Appl Catal A 2004; 262: 207–214.

(12) Aguayo AT, Ereña J, Sierra I, Olazar M, Bilbao J. Deactivation and regeneration of hybrid catalysts in the single-step synthesis of dimethyl ether from syngas and CO_2. Catal Today 2005; 106: 265-270.

(13) Dang S, Yang H, Gao P, Wang H, Li X, Wei W, Sun Y. A review of research progress on heterogeneous catalysts for methanol synthesis from carbon dioxide hydrogenation. Catal Today 2019; 330: 61–75.

(14) O.S. Joo, K.D. Jung, Il Moon, A. Y. Rozovskii, G. I. Lin, S.H. Han, and S. J. Uhm. Carbon dioxide hydrogenation to form methanol via a reverse-water-gas-shift reaction (the CAMERE Process). Ind. Eng. Chem. Res. 1999; 38: 1808–1812.

(15) B. Anicic, P. Trop, D. Goricanec. Comparison between two methods of methanol production from carbon dioxide. Energy 2014; 77:279-289.

(16) Zachopoulos A, Heracleous E. Overcoming the equilibrium barriers of CO_2 hydrogenation to methanol via water sorption: A thermodynamic analysis. J CO2 Util 2017; 21: 360–367.

(17) Gallucci F, Paturzo L, Basile A. An experimental study of CO_2 hydrogenation into methanol involving a zeolite membrane reactor. Chem Eng Process 2004; 43: 1029–1036.

(18) Gallucci F, Basile A. A theoretical analysis of methanol synthesis from CO_2 and H_2 in a ceramic membrane reactor. Int J Hydrogen Energy 2007; 32: 5050–5058.

(19) Atsonios K, Panopoulos KD, Kakaras E. Thermocatalytic CO_2 hydrogenation for methanol and ethanol production: Process improvements. Int J Hydrogen Energy 2016; 41: 792–806.

(20) Gorbe J, Lasobras J, Francés E, Herguido J, Menéndez M，Kumakiri I，Kita H. Preliminary study on the feasibility of using a zeolite A membrane in a membrane reactor for methanol production. Sep Purif Technol. 2018; 200: 164–168.

(21) Zhou C, Wang N, Qian Y, Liu X, Caro J, Huang A. Efficient synthesis of dimethyl ether from methanol in a bifunctional zeolite membrane reactor. Angew. Chem. Int. Ed. 2016; 55: 12678–12682.

(22) Iliuta I, F. Larachi F, Fongarland P. Dimethyl ether synthesis with in situ H_2O removal in fixed-bed membrane reactor: model and simulations. Ind Eng Chem Res 2010; 49: 6870–6877.

(23) Diban N, Urtiaga AM, Ortiz I, Ereña J, Bilbao J, Aguayob AT. Influence of the membrane properties on the catalytic production of dimethyl ether with in situ water removal for the successful capture of CO_2. Chem Eng J 2013; 234: 140–148.

(24) Falco MD, Capocelli M, Giannattasio A. Membrane Reactor for one-step DME synthesis process: Industrial plant simulation and optimization. J CO2 Util 2017; 22: 33–43.

(25) Catarina Faria A, Miguel CV, Madeira LM. Thermodynamic analysis of the CO_2 methanation reaction with in situ water removal for biogas upgrading. J CO2 Util 2018; 26: 271–280.

(26) Dehghani Z, Bayat M, Rahimpour MR. Sorption-enhanced methanol synthesis: Dynamic modeling and optimization. J Taiwan Inst Chem Eng 2014; 45:1490–1500.

(27) Arora A, Iyer SS, Bajaj I, Hasan MMF. Optimal Methanol Production via Sorption-Enhanced Reaction Process. Ind Eng Chem Res 2018; 57: 14143–14161.

(28) Iliuta I, Iliuta MC, Larachi F. Sorption-enhanced dimethyl ether synthesis—Multiscale reactor modeling. Chem Eng Sci 2011; 66:2241–2251.

(29) Borgschulte A, Gallandat N, Probst B, Suter R, Callini E, Ferri D, Arroyo Y, Erni R, Geerlings H, Zuttel A. Sorption enhanced CO_2 methanation. Phys Chem Chem Phys 2013; 15: 9620–9625.

(30) Carvill BT, Hufton JR, Anand M, Sircar S. Sorption-enhanced reaction process. AICHE J 1996; 42: 2765–2772.

(31) Jung S, Reining S, Schindler S, Agar DW. Application of Adsorptive Reactors for the Reverse Water Gas Shift Reaction. Chem Ing Tech 2013; 85: 484–488.

(32) Ghodhbene M, Bougie F, Fongarland P, Iliuta MC. Hydrophilic zeolite sorbents for in-situ water removal in high temperature processes. Can J Chem Eng 2017; 95: 1842–1849.

(33) Ness HCV, Abbott MM. Thermodynamics. In: R.H. Perry, D.W. Green. Perry's Chemical Engineers' Handbook, eighth ed. New York: McGraw-Hill; 2008. p. 4–28.

(34) Cui X, Kær SK. Thermodynamic analysis of steam reforming and oxidative steam reforming of propane and butane for hydrogen production. Int J Hydrogen Energy 2018; 43: 13009–13021.

(35) Kaiser P, Unde RB, Kern C, Jess A. Production of liquid hydrocarbons with CO_2 as carbon source based on reverse Water-gas shift and Fischer-Tropsch synthesis. Chem Ing Tech 2013; 85:489–499.

(36) Daza YA, Kuhn JN. CO2 conversion by reverse water gas shift catalysis: comparison of catalysts, mechanisms and their consequences for CO2 conversion to liquid fuels. RSC Adv 2016; 6: 49675–49691.

(37) Smith RJB, Loganathan M, Shantha MS. A Review of the Water Gas Shift Reaction Kinetics. Int J Chem React Eng 2010; 8: 1–32.

(38) Løvik, I. 2001. Modeling, estimation and optimization of the methanol synthesis with catalyst deactivation. Ph.D. Thesis, Norwegian University of Science and Technology.

(39) Klier K, Chatikavanij V, Herman RG, Simmons GW. Catalytic synthesis of methanol from CO/H_2: IV. The effects of carbon dioxide. J Catal 1982; 74: 343–360.

(40) Kung HH. Deactivation of methanol synthesis catalysts - a review. Catal Today 1992. 11: 443–453.

(41) Stangeland K, Li H, Yu Z. Thermodynamic Analysis of chemical and phase equilibria in CO_2 hydrogenation to methanol, dimethyl ether, and higher alcohols. Ind Eng Chem Res 2018; 57: 4081–4094.

(42) Samimi F, Karimipourfard D, Rahimpour MR. Green methanol synthesis process from carbon dioxide via reverse water gas shift reaction in a membrane reactor. Chem Eng Res Des 2018; 140:44–67.

Table of Contents (TOC)/Abstract Graphic

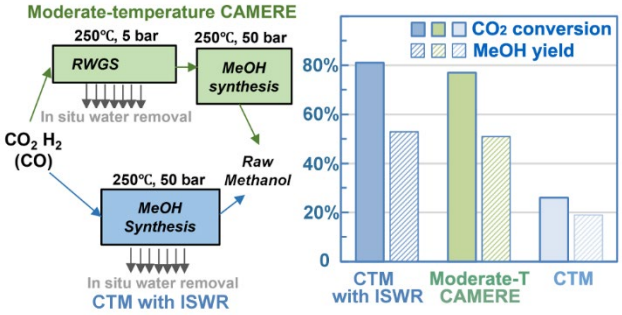

Supporting Information

Thermodynamic Analyses of a Moderate-Temperature Process of Carbon Dioxide Hydrogenation to Methanol via Reverse Water−Gas Shift with In Situ Water Removal

Xiaoti Cui*, Søren Knudsen Kær

Department of Energy Technology, Aalborg University, 9220 Aalborg, Denmark

*Corresponding author:

Xiaoti Cui

Tel: +45 2667 8192;

E-mail: xcu@et.aau.dk;

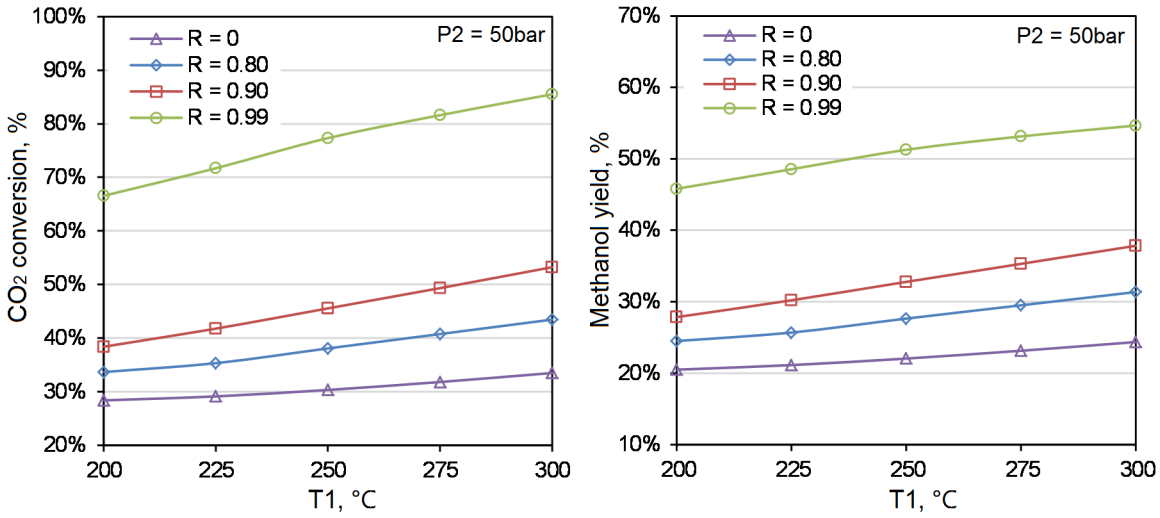

(a) (b)

Figure S1. Equilibrium (a) CO_2 conversion and (b) methanol yield for the CAMERE process at different *T1* and *R* values (for the RWGS part) and *P2* = 50 bar for the MeOH synthesis part.

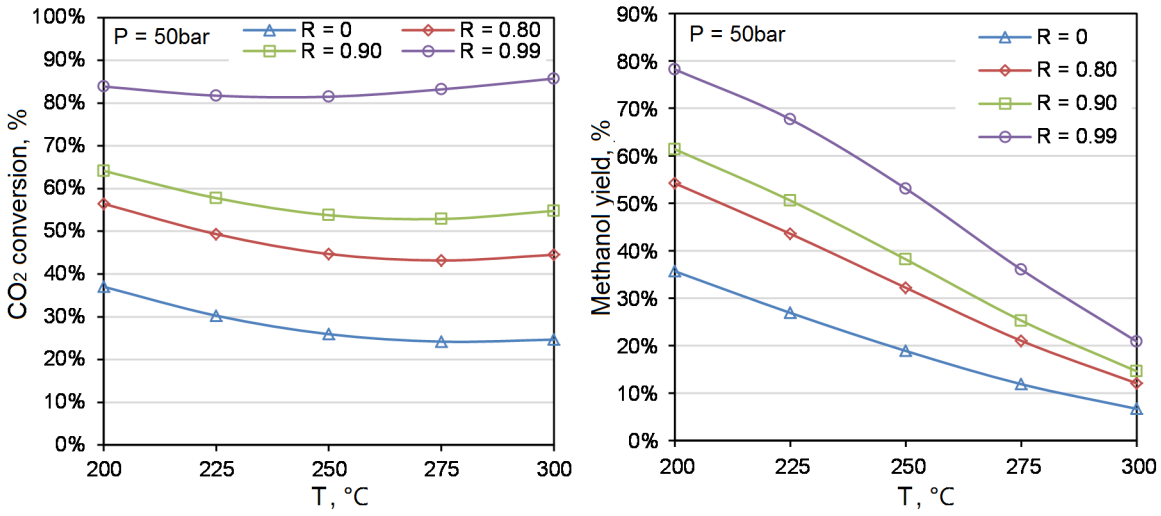

(a) (b)

Figure S2. Equilibrium (a) CO_2 conversion and (b) methanol yield for the CTM process under the conditions with H_2/CO_2 = 3 (feed gas), T = 200 – 300 ℃, P = 50 bar and R = 0 – 0.99.

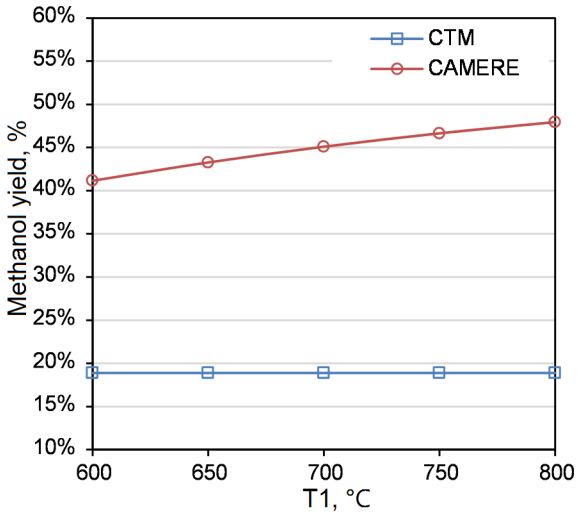

Figure S3. Equilibrium methanol yield under the conditions of H_2/CO_2 = 3, *T2* = 250°C, *P2* = 50 bar, *P*1= 5 bar and *T1* = 600°C – 800°C for the high-temperature CAMERE process and H_2/CO_2 = 3, *T* = 250°C, *P* = 50 bar for the CTM process.

Table S1. The calculated values of Z and SF_Z for Figure 2*.

			R = 0.8		
	200℃	225℃	250℃	275℃	300℃
Z	3	3	3	2	2
SF_Z	0.151	0.100	0.035	0.976	0.926
			R = 0.9		
Z	5	5	5	4	4
SF_Z	0.400	0.250	0.075	0.905	0.750
			R = 0.99		
Z	33	30	28	24	21
SF_Z	1.000	0.700	0.140	0.400	0.550

* the values in the table are also used for Figure 5, Figure 6, Figure 9 and Figure S1.

Table S2. The calculated values of Z and SF_Z for Figure 3a*.

				R = 0.8				
H_2/CO_2	1	2	3	4	5	6	7	8
Z	3	3	3	2	2	2	2	2
SF_Z	0.160	0.120	0.035	1.000	0.980	0.960	0.940	0.916
				R = 0.9				
Z	5	5	5	4	4	4	4	4
SF_Z	0.230	0.170	0.075	0.983	0.905	0.835	0.768	0.705
				R = 0.99				
Z	33	31	28	25	23	22	20	19
SF_Z	0.070	0.080	0.140	0.800	1.000	0.200	0.800	0.600

*: the values in the table are also used for Figure 7a.

Table S3. The calculated values of Z and SF_Z for Figure 3b*.

				R = 0.8			
$CO/(CO+CO_2)$	0	0.1	0.2	0.3	0.4	0.5	0.6
Z	3	3	3	3	4	4	4
SF_Z	0.350	0.360	0.650	0.895	0.120	0.310	0.460
				R = 0.9			
Z	5	5	6	6	7	7	8
SF_Z	0.075	0.633	0.172	0.710	0.195	0.645	0.030
				R = 0.99			
Z	28	29	32	35	38	41	43
SF_Z	0.140	0.500	0.700	0.900	0.500	0.010	0.500

*: the values in the table are also used for Figure 7b.

Table S4. The calculated values of Z and SF_Z for Figure 11 and Figure S2.

R = 0.8, P = 30 bar					
	200℃	225℃	250℃	275℃	300℃
Z	2	2	2	2	2
SF_Z	0.724	0.834	0.9025	0.9225	0.9055
R = 0.9, P = 30 bar					
Z	4	4	4	4	4
SF_Z	0.123	0.477	0.690	0.747	0.690
R = 0.99, P = 30 bar					
Z	18	22	23	22	21
SF_Z	0.600	0.200	0.200	0.800	0.150
R = 0.8, P = 50 bar					
Z	2	2	2	2	2
SF_Z	0.5395	0.675	0.781	0.848	0.868
R = 0.9, P = 50 bar					
Z	3	3	4	4	4
SF_Z	0.668	0.977	0.315	0.520	0.578
R = 0.99, P = 50 bar					
Z	13	16	19	20	20
SF_Z	0.900	1.000	0.500	0.800	0.300
R = 0.8, P = 70 bar					
Z	2	2	2	2	2
SF_Z	0.3955	0.5485	0.6745	0.7685	0.821
R = 0.9, P = 70 bar					
Z	3	3	3	4	4
SF_Z	0.347	0.690	0.977	0.275	0.435
R = 0.99, P = 70 bar					
Z	12	13	17	18	19
SF_Z	0.300	0.800	0.200	0.700	0.200

Table S5. The calculated values of Z and SF_Z for Figure 12a.

				R = 0.8				
H_2/CO_2	1	2	3	4	5	6	7	8
Z	2	2	2	2	2	2	2	2
SF_Z	0.849	0.808	0.781	0.752	0.718	0.6816	0.646	0.6084
				R = 0.9				
Z	4	4	4	4	4	3	3	3
SF_Z	0.595	0.416	0.315	0.200	0.064	0.942	0.842	0.746
				R = 0.99				
Z	27	22	19	16	14	12	11	10
SF_Z	0.330	0.700	0.500	0.700	0.350	0.500	0.150	0.150

Table S6. The calculated values of Z and SF_Z for Figure 12b.

			R = 0.8				
$CO/(CO+CO_2)$	0	0.1	0.2	0.3	0.4	0.5	0.6
Z	2	2	3	3	3	3	3
SF_Z	0.781	0.920	0.100	0.319	0.538	0.764	0.984
			R = 0.9				
Z	4	4	4	5	5	6	6
SF_Z	0.315	0.622	0.943	0.350	0.780	0.269	0.808
			R = 0.99				
Z	19	20	22	24	26	29	32
SF_Z	0.500	0.900	0.450	0.400	0.500	0.600	0.250